SSSAJ

Soil Science Society of America Journal

Vol. 68 No. 3 May–June 2004

SSSJD4 68(3):713–1130 (2004)

SOIL SCIENCE SOCIETY OF AMERICA JOURNAL

Business and Editorial Offices at
677 South Segoe Road, Madison, WI 53711
(www.soils.org)

Published bimonthly by the Soil Science Society of America, Inc. Periodicals postage paid at Madison, WI, and at additional mailing offices.

Postmaster: Send address change to *SSSA Journal*, 677 S. Segoe Rd., Madison, WI 53711.

Subscription rates (nonmember): $600 per year, within the USA; all others $636. Single copies, $33 USA; elsewhere, $39. Members are eligible for reduced subscription rates. New subscriptions, renewals, and new memberships that include the *SSSA Journal* begin with the first issue of the current year. Claims for copies lost in the mail must be received within 90 days of publication date for domestic subscribers, and within 26 weeks of publication date for foreign subscribers.

Membership in the Society is not a requirement for publication in *SSSA Journal*; however, nonmembers will be charged an additional amount for the first six published pages of a manuscript. To qualify for member rates, at least one author must be an active, emeritus, graduate student, or undergraduate student member of SSSA, CSSA, or ASA on the date the manuscript is accepted for publication.

Volunteered papers will be assessed a manuscript charge of $650 for members and $750 for nonmembers. No charge will be assessed against comments and letters to the editor. The Society absorbs the cost of reproducing illustrations up to $15 for each paper.

Contributions to the *SSSA Journal* may be (i) papers and notes on original research; and (ii) "Comments and Letters to the Editor" containing (*a*) critical comments on papers published in one of the Society outlets or elsewhere, (*b*) editorial comments by Society officers, or (*c*) personal comments on matters having to do with soil science. Letters to the Editor are limited to one printed page. Contributions need not have been presented at annual meetings. Original research findings are interpreted to mean the outcome of scholarly inquiry, investigation, or experimentation having as an objective the revision of existing concepts, the development of new concepts, or the improvement of techniques in some phase of soil science. Short, critical reviews or essays on timely subjects, upon invitation by the Editorial Board, may be published on a limited basis. Refer to SSSA Publication Policy (Soil Sci. Soc. Am. J. 64(1):1–3, 2000) and to the *Publications Handbook and Style Manual* (ASA-CSSA-SSSA, 1998).

Keep authors anonymous from reviewers by listing title, author(s), author–paper documentation, and acknowledgments on a detachable title page. Repeat manuscript title on the abstract page.

Manuscripts are to be sent to Dr. Richard L. Mulvaney, Editor, *SSSA Journal*, University of Illinois, 1102 South Goodwin Avenue, Urbana, IL 61801 (email: mulvaney@uiuc.edu). Four copies of the manuscript on line-numbered paper are required. All other correspondence should be directed to the Managing Editor, 677 S. Segoe Rd., Madison, WI 53711.

Trade names are sometimes listed in papers in this journal. No endorsement of these products by the publisher is intended, nor is any criticism implied of similar products not mentioned.

ISSN 0361-5995

SSSAJ May–June 2004 Vol. 68, No. 3

Soil Science Society of America Journal

Continued on page ii

This issue's cover: Reforesting reclaimed mined land in Virginia. See p. 833–844, "Forest Soil Productivity of Mined Land in the Midwestern and Eastern Coalfield Regions," by J.A. Rodrigue and J.A. Burger. Photo by Rick Williams.

Continued from page i

SOIL SCIENCE SOCIETY OF AMERICA
JOURNAL

VOL. 68 MAY–JUNE 2004 No. 3

DIVISION S-1—SOIL PHYSICS

A Simple Method for Estimating Water Diffusivity of Unsaturated Soils

Quanjiu Wang, Mingan Shao, and Robert Horton*

ABSTRACT

Numerical models have been extensively used for predicting water and solute transport in saturated and unsaturated soils. Soil hydraulic properties are required for quantitatively describing water and chemical transport processes in soils by the numerical models. Soil water diffusivity is one of the important hydraulic properties. Several approaches have been developed to estimate the soil water diffusivity, however the intensive calculations and time-consuming measurements required by the methods for determining soil water diffusivity limit the application of the methods. It is necessary to develop a method with easily performed experiments for determining soil water diffusivity. In this paper, the problem of water absorption into a horizontal soil column is solved, and the relationship between cumulative infiltration and infiltration rate with the distance of the wetting front are obtained. Based on the relationships, a new and relatively simple method for estimating soil water diffusivity is presented in this paper. Experiments of water absorption into 60-cm long and 25-cm long horizontal soil columns were conducted to evaluate the method. Estimates of soil water diffusivity by the new method were in good agreement with estimates by the Bruce and Klute method. With the new method short (approximately 8 cm) soil columns can be used, and it is possible to use the new method to estimate soil water diffusivity of undisturbed soils. Therefore, the present method provides simplicity for determining soil water diffusivity.

MATHEMATICAL MODELS have been used in research and management to predict water and solute transfer in soil and ground water. The accuracy of water flow and solute transport predictions obtained with the models depends to a large extent on the reliability and accuracy of the soil hydraulic properties. The required hydraulic properties are hydraulic conductivity, water diffusivity, and specific water capacity (Bohne et al., 1995). Among the three parameters, only two of them are independent.

In recent years, there have been increased efforts to estimate soil water diffusivities of unsaturated soils, as one of the major soil hydraulic properties. Usually horizontal infiltration experiments have been used to relate soil water diffusivity to the volumetric water content by the method of Bruce and Klute (1956). The method is based on the Boltzmann transformation. The slope of the water content distribution curve along the soil column needs to be measured to estimate the water diffusivity. Kirkham and Powers (1972) described in detail this common method for estimating soil water diffusivity. However, it is difficult to exactly determine the slope of the water content distribution curve, and thus the difficult estimation of the slope of the water content distribution leads to soil water diffusivity estimation error. Cassel et al. (1968) presented a method for estimating soil water diffusivity from time-dependent soil water content distributions in the horizontal redistribution process. Their method requires measuring water content distribution with time and also involves both relatively intensive calculation and time-consuming experiments. Clothier et al. (1983) presented a fitting function chosen from those presented by Philip (1960) to approximate the water distribution curve in the Bruce and Klute (1956) method. This made possible a simple analytical expression of the water diffusivity by avoiding finding the slopes of the soil water distribution curve. However, the fitting function of Clothier et al. (1983) may not apply to all soils. McBride and Horton (1985), based on the Bruce and Klute (1956) method, developed a method of determining the water diffusivity from horizontal infiltration experiments. However the method involves intensive calculations. Warrick (1994) gave a detailed review on soil water diffusivity estimation for fixed water content at the inlet boundary. Shao and Horton (1996) developed a method to estimate the soil water diffusivity by using a nonhysteretic analytical solution to horizontal redistribution based on general similarity

Q. Wang, State Key Laboratory of Soil Erosion and Dryland Farming on the Loess Plateau, Institute of Soil and Water Conservation, Chinese Academy of Sciences, Yangling, 712100; Institute of Water Resources Research, Xi'an University of Technology, Xi'an 710048, China; Q. Wang and M. Shao, Institute of Geographical Sciences and Natural Resources Research (Beijing 100101) and Institute of Soil and Water Conservation (Yangling, 712100) of Chinese Academy of Sciences, China; R. Horton, Dep. of Agronomy, Iowa State University, Ames, IA 50011. Received 26 Feb. 2003. *Corresponding author (rhorton@iastate.edu).

Published in Soil Sci. Soc. Am. J. 68:713–718 (2004).

677 S. Segoe Rd., Madison, WI 53711 USA

theory. The method only requires information on the advance of the wetting front with time to obtain the soil water diffusivity in the process of water redistribution. Shao and Horton (1996) assumed a power function between the soil water diffusivity and the soil water content, however the form of their power function may not apply to all soils. A power function relationship between soil water diffusivity and relative water content may have a more general application to soils than does the Shao and Horton (1996) power function relationship.

The purpose of the present paper is to develop a method for determining the water diffusivity of unsaturated soils. To obtain an analytical expression of the diffusivity, the problem of water absorption into a horizontal soil column is solved. The relationships among cumulative infiltration and infiltration rate and the wetting front are obtained. With these relationships the soil water diffusivity as a function of relative water content can easily be determined. Three soils were used to evaluate the method. This paper compares analytical values of the soil water diffusivity with those obtained by the method of Bruce and Klute (1956).

THEORY

Darcy's equation describing one-dimensional horizontal flow of water in unsaturated soil is

$$q = k(h)\frac{dh}{dx} = -D(\theta)\frac{d\theta}{dx} \quad [1]$$

where q is soil water flux (cm min^{-1}), $k(h)$ is unsaturated hydraulic conductivity (cm min^{-1}), h is soil–water suction (cm), x is the horizontal distance (cm), $D(\theta)$ is the soil water diffusivity (cm^2 min^{-1}), and θ is the soil water content (cm^3 cm^{-3}).

The following equation was used to describe the unsaturated conductivity (Brooks and Corey, 1964)

$$k(h) = k_s\left(\frac{h_d}{h}\right)^m \quad [2]$$

where k_s is saturated conductivity (cm min^{-1}), h_d is air-entry suction (cm), and m is a constant.

The soil water retention curve (Brooks and Corey, 1964) is

$$\frac{\theta - \theta_r}{\theta_s - \theta_r} = \left(\frac{h_d}{h}\right)^n \quad [3]$$

where θ_s is the saturated soil water content (cm^3 cm^{-3}), θ_r is the residual water content (cm^3 cm^{-3}), n is a parameter, and the left hand ratio is equal to the relative water content, S.

For the water absorption problem of one-dimensional horizontal soil column, the general equation and the initial and boundary conditions are

$$\begin{aligned} \frac{\partial\theta}{\partial t} &= \frac{\partial}{\partial x}\left(D\frac{\partial\theta}{\partial x}\right) \\ \theta(x,0) &= \theta_i \\ \theta(0,t) &= \theta_s \\ \theta(\infty,t) &= \theta_i \end{aligned} \quad [4]$$

where θ_i is the initial soil water content (cm^3 cm^{-3}).

Integrating Eq. [4] with respect to θ gives,

$$\int_\theta^{\theta_s}\frac{\partial x}{\partial t}d\theta + D(\theta_s)\left[\frac{\partial\theta}{\partial x}\right]_s - D(\theta)\frac{\partial\theta}{\partial x} = 0 \quad [5]$$

Parlange (1971) considered that the first term in Eq. [5] is small compared with the rest of the terms in Eq. [5] and may be neglected when soil water content is close to the saturated water content. Eq. [5] reduces to:

$$D(\theta_s)\left[\frac{\partial\theta}{\partial x}\right]_s \approx D(\theta)\frac{\partial\theta}{\partial x} \quad [6]$$

We can let

$$i = -D(\theta_s)\left[\frac{\partial\theta}{\partial x}\right]_s \quad [7]$$

Because the right side in Eq. [7], describing the soil water flux at the soil surface, is actually infiltration rate, i, Eq. [6] becomes

$$i = -D(\theta)\frac{\partial\theta}{\partial x} \quad [8]$$

Converting Eq. [8] as

$$i = k(h)\frac{dh}{dx} \quad [9]$$

Then Eq. [9] can be integrated and converted as follows

$$ix = \frac{h_d^m k_s}{1-m}(h_x^{1-m} - h_d^{1-m}) \quad [10]$$

where h_x is the suction at the x position. If the initial water content is relatively small and h_x is relatively large, h_x^{1-m} is very small at the wetting front, $x = x_f$, and x_f is the wetting front distance and can be observed visually. Therefore Eq. [10] can be simplified

$$ix_f = \frac{h_d^m k_s}{1-m}(-h_d^{1-m}) = \frac{h_d k_s}{m-1} \quad [11]$$

and i is expressed as

$$i = \frac{1}{x_f}\frac{h_d k_s}{m-1} \quad [12]$$

Equation [8] actually assumes that the flux is only a function of time, and Eq. [12] expresses the relationship between the infiltration rate and the wetting front distance. The infiltration rate decreases with the advance of the wetting front.

Combining Eq. [10] with [12], a new relation is found

$$\frac{x}{x_f} = 1 - \left(\frac{h_d}{h_x}\right)^{m-1} \quad [13]$$

The suction, h_x, at a distance, x, can be calculated by Eq. [13]. Combining Eq. [3] with [13] the soil water content at a distance, x, can also be expressed as

$$\frac{x_f - x}{x_f} = \left(\frac{\theta_x - \theta_r}{\theta_s - \theta_r}\right)^{\frac{m-1}{n}} \quad [14]$$

The cumulative infiltration to the wetting front can be expressed as

$$I = \int_{\theta_i}^{\theta_s} x\,d\theta \quad [15]$$

Combining Eq. [14] with [15], the cumulative infiltration is as follows

$$I = x_f(\theta_s - \theta_i) - \frac{nx_f}{m+n-1}(\theta_s - \theta_r)^{\frac{1-m}{n}} \left[(\theta_s - \theta_r)^{\frac{m+n-1}{n}} - (\theta_i - \theta_r)^{\frac{m+n-1}{n}}\right] \quad [16]$$

If the initial water content (air-dried soil) is small, and the

residual water is considered to equal the initial water content, the cumulative infiltration is

$$I = x_f(\theta_s - \theta_i)\left[\frac{1}{1 + n/(m-1)}\right] \quad [17]$$

Equation [17] shows that the cumulative infiltration is a linear function of the distance to the wetting front.

The infiltration rate is the differential rate of the cumulative infiltration

$$\frac{dI}{dt} = i \quad [18]$$

Combining Eq. [18] with [17] and [12]

$$x_f = \sqrt{\frac{2h_d k_s(m + n - 1)}{(m^2 - 1)(\theta_s - \theta_i)}}\, t^{1/2} \quad [19]$$

Equation [19] shows the relationship between time and the wetting front distance. Combining Eq. [14] with Eq. [19]

$$x = \sqrt{\frac{2h_d k_s(m + n + 1)}{(m^2 - 1)(\theta_s - \theta_i)}}\left[1 - \left(\frac{\theta - \theta_i}{\theta_s - \theta_i}\right)^{\frac{m-1}{n}}\right] t^{1/2} \quad [20]$$

Let

$$Q(\theta) = \left[1 - \left(\frac{\theta - \theta_i}{\theta_s - \theta_i}\right)^{\frac{m-1}{n}}\right]\sqrt{\frac{2h_d k_s(m + n - 1)}{(m^2 - 1)(\theta_s - \theta_i)}}$$

Hence

$$x = Q(\theta)t^{1/2} \quad [21]$$

The well-known Boltzmann transform equation is $x(\theta,t) = \lambda(\theta)t^{1/2}$, and Eq. [21] is similar in form to the expression of the Boltzmann transform.

Soil water diffusivity can be expressed as a function of soil water retention curve and unsaturated soil water conductivity curve

$$D = -k\frac{dh}{d\theta} \quad [22]$$

The soil water diffusivity may be described as a power function of relative water content, as follows for a Brooks–Corey (Brooks and Corey, 1964) soil

$$D = D_s\left(\frac{\theta - \theta_r}{\theta_s - \theta_r}\right)^L \quad [23]$$

where D_s is the diffusivity of saturated soil and L is a parameter.

Combining Eq. [2] and [3] with Eq. [22] gives

$$D = \frac{k_s h_d}{n(\theta_s - \theta_i)}\left(\frac{\theta - \theta_i}{\theta_s - \theta_i}\right)^{\frac{m-n-1}{n}} \quad [24]$$

To obtain the related parameters in Eq. [24], Eq. [24] can be rearranged as

$$D = \left(\frac{m-1}{n}\right)\frac{k_s h_d}{(m-1)(\theta_s - \theta_i)}\left(\frac{\theta - \theta_i}{\theta_s - \theta_i}\right)^{\frac{m-1}{n}-1} \quad [25]$$

Hence

$$D_s = \frac{m-1}{n}\frac{k_s h_d}{(m-1)(\theta_s - \theta_r)} \quad [26]$$

$$L = \frac{m-1}{n} - 1 \quad [27]$$

$(m-1)/n$ in Eq. [26] and [27] can be calculated based on Eq. [17], and $k_s h_d/(m-1)$ in Eq. [26] can be estimated based on Eq. [12]. Therefore, when the relations of the infiltration rate and the cumulative infiltration with the wetting front distance are known, the soil water diffusivity can be easily estimated.

To get even easier parameter expressions, Eq. [12] and [17] are expressed as follows:

$$i = \frac{a}{x_f} \quad [28]$$

$$I = bx_f \quad [29]$$

Where

$$a = \frac{h_d k_s}{m-1} \quad [30]$$

$$b = (\theta_s - \theta_i)\left[\frac{1}{1 + n/(m-1)}\right] \quad [31]$$

Hence D_s and L can be expressed as follows:

$$D_s = \frac{a}{\theta_s - \theta_i}\Big/\left(\frac{\theta_s - \theta_i}{b} - 1\right) \quad [32]$$

$$L = 1\Big/\left(\frac{\theta_s - \theta_r}{b} - 1\right) - 1 \quad [33]$$

When a and b are obtained through the analysis of experimental data, the parameters D_s and L can be estimated with Eq. [32] and [33]. Then the soil water diffusivity can be readily determined by Eq. [24].

MATERIALS AND METHODS

One-dimensional water absorption experiments for horizontal soil columns were performed to evaluate the new method. Experiments were conducted using a horizontal cylindrical column with a length of 60 cm and a diameter of 9 cm to measure soil water content by a γ radiation attenuation method. The relatively large soil column and the γ radiation attenuation method were used to accommodate the Bruce and Klute method. The new method did not require measurements of soil water content profiles. Three soils from Shaanxi province of China were used as the experimental materials. The soils were Yulin sand, Shuide loam and Xian silt loam, and the related physical properties of the three soils are listed in Table 1. Air-dried soils were passed through a 2-mm screen,

Table 1. Basic soil physical properties.

	Soil particle diameter				Bulk density	Initial water content
	<2 mm	<0.05 mm	<0.01 mm	<0.005 mm	g cm^{-3}	cm^3 cm^{-3}
Yulin	100	11.5	5.4	4.7	1.7	0.02
Shuide	100	44.1	19.5	12.7	1.4	0.02
Xian	100	69.7	59.3	8.0	1.35	0.02

and the columns were packed layer by layer with air-dried soils of a given soil bulk density. A Marriotte tube was used to supply water, and a zero water head was maintained at the soil inlet. The volume of infiltrated water was recorded with time. A γ radiation attenuation method (relative error <2% for volumetric water content) was used to measure soil water content profiles in 1-h intervals, to calculate the diffusivity by the Bruce and Klute (1956) method. The wetting front distance with time was observed visually based on obvious color differences at the interface of the wet and dry soil. The infiltration rate versus time was calculated based on the cumulative infiltration with time. Using the observed data of the cumulative infiltration versus time, the changes of infiltration rate and the wetting front distance with time, soil water diffusivities were calculated by the new analytical relationships presented in the theory section. The diffusivities of the three soils were also calculated with the Bruce and Klute method based on the measured soil water content profile.

It is convenient to use small soil columns to estimate soil water diffusivity. To indicate the effect of soil column size on the new method, a horizontal infiltration experiment with Yulin sand was also conducted using a column with a length

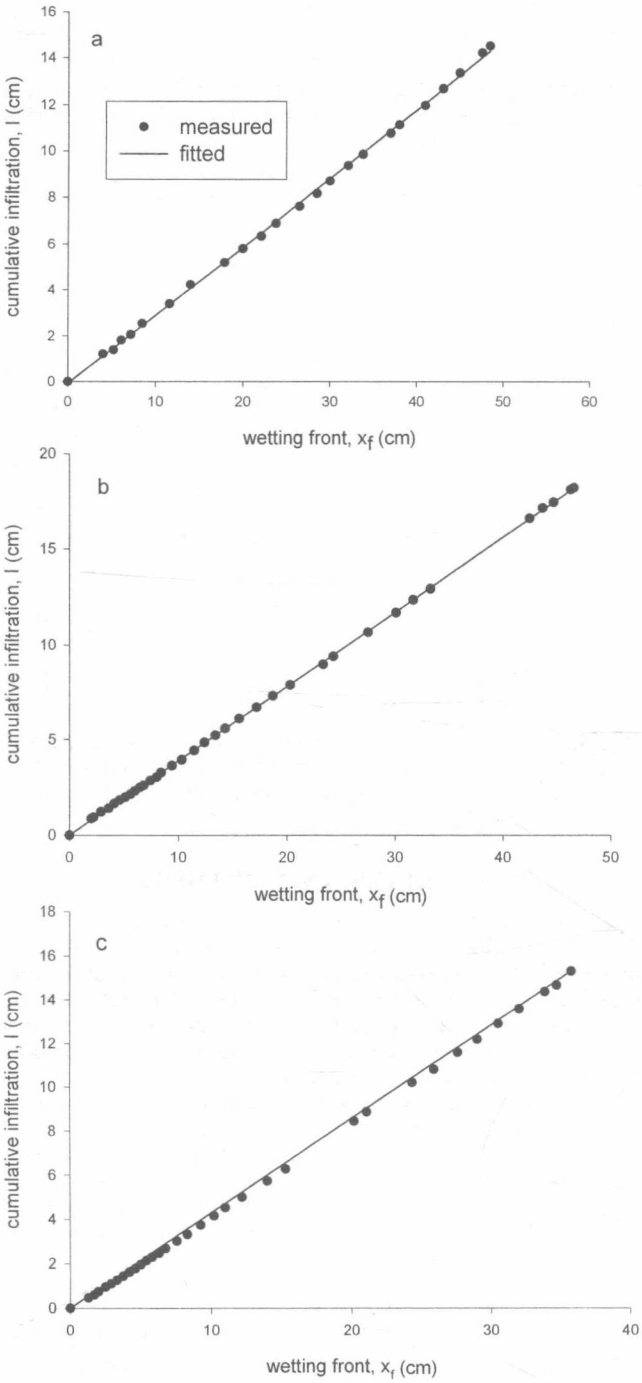

Fig. 1. Cumulative infiltration versus the wetting front distance for three soils ([a] Yulin Sand, [b] Shuide Loam, and [c] Xian Silt Loam).

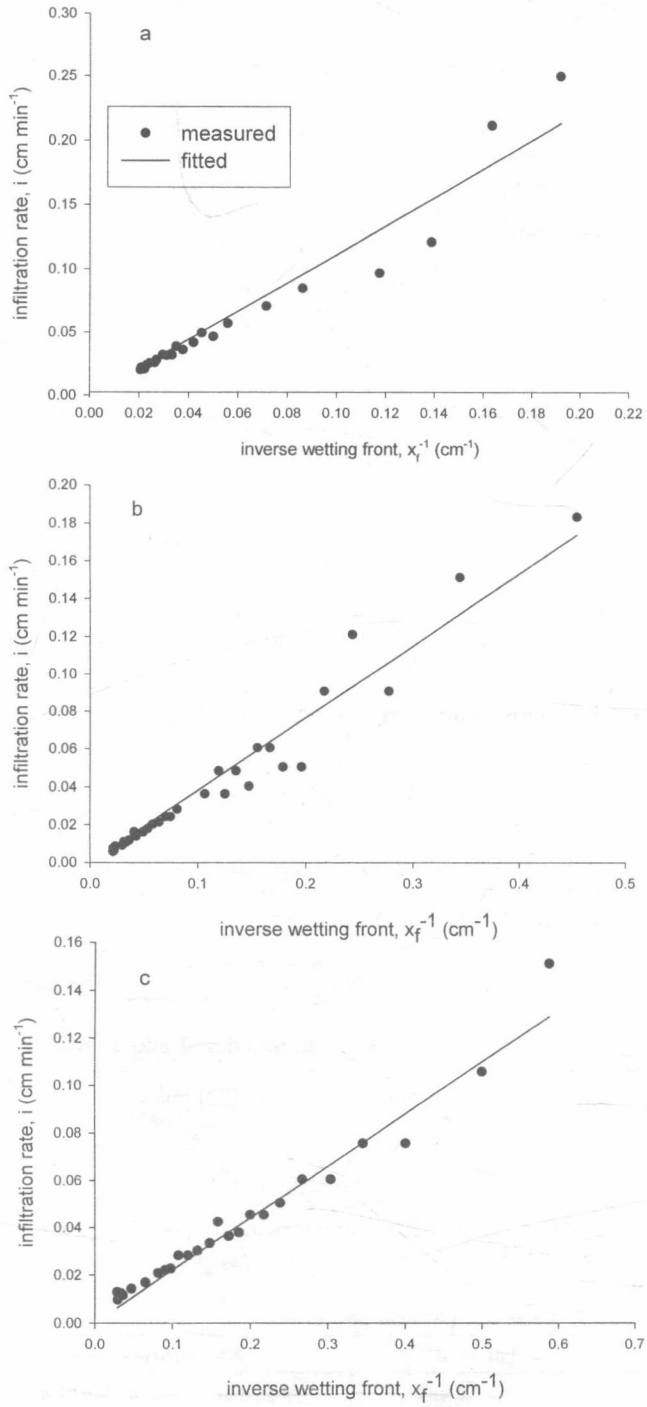

Fig. 2. Infiltration rate versus the inverse wetting front distance for three soils ([a] Yulin Sand, [b] Shuide Loam, and [c] Xian Silt Loam).

of 25 cm and a diameter of 4 cm. A Marriotte tube was used to supply water, and a zero water head was maintained at the soil inlet. The volume of infiltrated water was recorded with time. The wetting front distance with time was observed visually. The new method was used to estimate soil water diffusivity.

RESULTS

As mentioned above, to obtain soil water diffusivity of unsaturated soils, the advance of the wetting front with time, cumulative infiltration and infiltration rate are measured in the experiments. Figure 1 and 2 show the measured cumulative infiltration versus the wetting front distance and the infiltration rate versus the inverse wetting front distance, respectively, for each soil. Each data set is treated with Eq. [28] and [29]. The a and b parameters are related to D_s and L in Eq. [23], which describes the soil water diffusivity by a power function of relative water content. The a and b parameters are estimated by least squares regression of fitting the observed data of the cumulative infiltration versus the wetting front distance and the infiltration rate versus the inverse wetting front distance, respectively, for the soils, and the results are shown in Table 2. All of the coefficients of determination values, R^2, of the fitting are >0.97. Therefore it may be safe to say that Eq. [28] and [29] describe the relations of cumulative infiltration versus the wetting front distance and the infiltration rate versus the inverse wetting front distance well. The D_s and L in Eq. [23] are calculated by using Eq. [32] and [33], and the results are shown in Table 3. To evaluate the new method, the soil water diffusivity is also determined by the method of Bruce and Klute (1956), and the results are also listed in Table 3.

The soil water diffusivity of the new method is determined by Eq. [32] and [33]. Because the values of D_s and L are dependent on a and b constants in Eq. [28] and [29], it may be interesting to look at the sensitivities of soil water diffusivity to a and b coefficients in Eq. [28] and [29]. The D_s value depends on both a and b, but L only depends on b. When b increases, L also increases. For a given soil, saturated and initial water content are constant (here θ_s is assumed to 0.45 cm^3 cm^{-3}, and θ_i is 0.02 cm^3 cm^{-3}), a sensitivity analysis shows that L increases about 10 times when b increases from 0.3 to 0.4. The values listed in Table 2 and 3 also show that L increases as b increases. The value of L influences the shape of the curve of soil water diffusivity, thus the shape of the curve of soil water diffusivity is mainly affected by the value of b. We may know from Eq. [32] that D_s linearly increases as parameter a increases for given values of b and initial and saturated water contents. For given values of parameter a, initial and satu-

Table 2. The regression parameters for three soils.

	Yuling	Shuide	Xian
a	1.030	0.382	0.220
b	0.29	0.39	0.42
R_1^2	0.98	0.98	0.97
R_2^2	0.99	0.99	0.99

Where R_1^2 and R_2^2 are correlation coefficients for the infiltration rate with the inverse wetting front distance and the cumulative infiltration versus the wetting front distance, respectively.

Table 3. The estimated soil water diffusivity parameters for three soils.

Soil	Yuling	Shuide	Xian
D_{s1}, cm^2 min^{-1}	15.7	5.51	4.16
D_{s2}, cm^2 min^{-1}	14.5	6.05	4.50
L_1	3.35	5.49	8.09
L_2	3.29	5.37	8.03

Where D_{s1} and L_1 were estimated by the simple method, and D_{s2} and L_2 were obtained by the method of Bruce and Klute (1956).

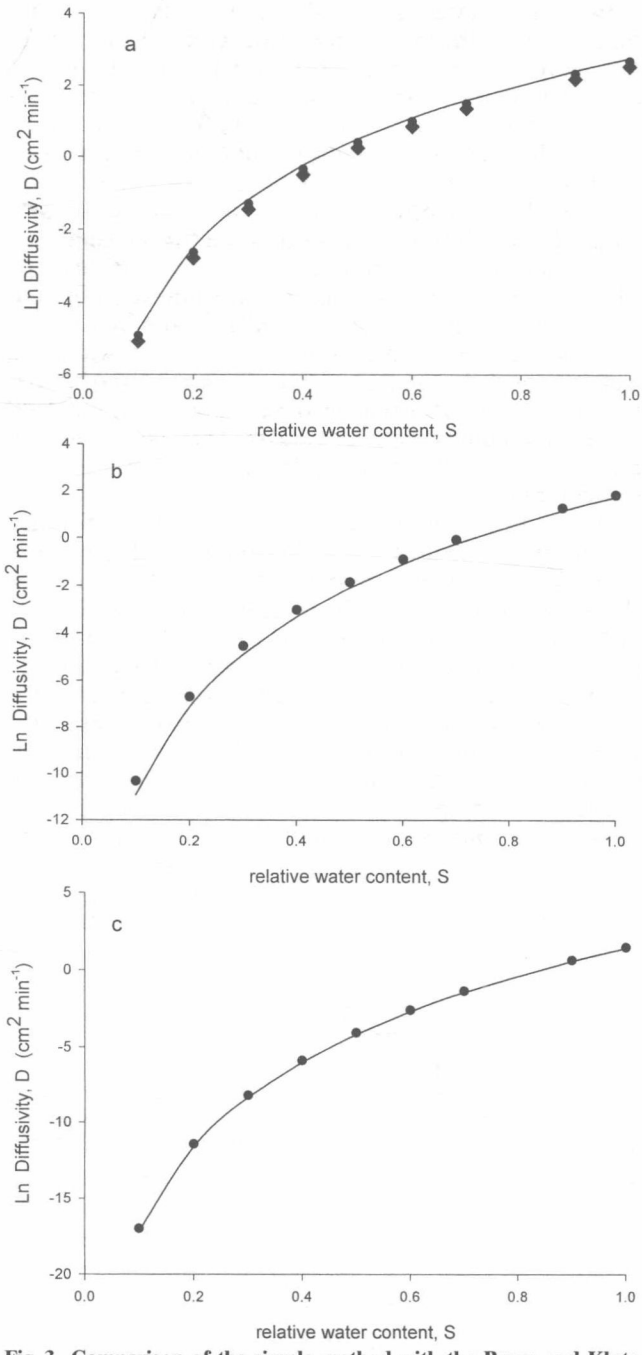

Fig. 3. Comparison of the simple method with the Bruce and Klute method ([a] Yulin Sand, [b] Shuide Loam, and [c] Xian Silt Loam; the solid points represent the Bruce and Klute method, the solid curves represent the new method for large soil columns, and the diamonds the new method for a small soil column).

rated water content, D_s increases as b decreases. In addition, because D_s determines the magnitude of the diffusivity function, the magnitude of the diffusivity is affected by both parameters, a and b.

The values of soil water diffusivity estimated by the simple approach are compared with those obtained by the method of Bruce and Klute (1956), and the results are shown in Fig. 3. The results indicate that the water diffusivity estimated by the simple method is very close to the values obtained by the method of the Bruce and Klute (1956). The Root Mean Square Error (RMSE) between the values estimated by the simple method and those obtained by the method of Bruce and Klute (1956) are analyzed. The values of the RMSE for three soils, from Yuling sand, Shuide loam, and Xian silt loam of Shaanxi in China, are 0.54, 0.18, and 0.13, respectively. The small RMSE values indicate that the simple method can be effectively used to estimate soil water diffusivity.

To analyze the effect of soil column size on the new method, the infiltration data observed for the small soil column are used to estimate the soil water diffusivity. The parameters a and b for Yulin sand are 1.00 and 0.28, respectively; and the D_s and L, estimated by the new method, are 12.5 and 3.3, respectively, when the wetting front distance is 15 cm. Figure 3a shows that the soil water diffusivity estimated by the small and large soil columns are very similar. The results indicate that the new method is applicable to relatively small soil columns.

To analyze the influence of the wetting front distance on the soil water diffusivity, the soil water diffusivity is also calculated with different wetting front distance, as shown in Fig. 4. The results indicate that the soil water diffusivity calculated at a wetting front distance of 10 cm is nearly identical to that for a wetting front distance of 15 cm. Likewise, soil water diffusivity calculated for a wetting front distance of 8 cm is similar to those for wetting front distances of 10 and 15 cm. When the wetting front is <8 cm, soil water diffusivity differs from the 15-cm wetting front values of soil water diffusivity. This analysis implies that the new method may be applied to soil columns having a minimum wetting front length of 8 cm.

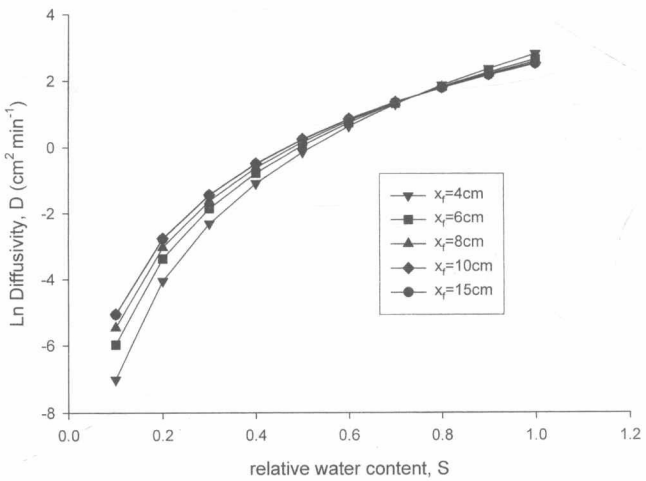

Fig. 4. Estimated soil water diffusivities for different wetting front distances in a soil column.

CONCLUSIONS

Soil water diffusivity is one of the important hydraulic properties affecting water and solute transport rates in soils. It is necessary to develop a simple method to determine soil water diffusivity because the current methods have limitations. In this paper a simple method has been developed to determine the water diffusivity of unsaturated soils. The problem of water absorption into a horizontal soil column is solved based on the assumption of Parlange (1971), and the relationships among cumulative infiltration with the wetting front distance and infiltration rate with the wetting front distance are analytically obtained. When the relationships are available, the soil water diffusivity can be readily estimated. Estimates of soil water diffusivity by the simple method are in good agreement with estimates by the Bruce and Klute method. The new method can be applied to disturbed or undisturbed soil columns with 8 cm or more wetting front length. The present method provides simplicity for determining soil water diffusivity. The method is applicable to laboratory determination of soil water diffusivity of unsaturated soils.

ACKNOWLEDGMENTS

This work was funded in part by the China National Natural Science Foundation (Project numbers: 90102012 and 40025106) and the key project of resources, ecological and environmental research of the Chinese Academy of Sciences (Project No: KZCX2-411), and this journal paper of the Iowa Agriculture and Home Economics Experiment Station, Ames, IA, Project No. 3287, was supported in part by Hatch Act and State of Iowa funds.

REFERENCES

Bohne, K., C. Roth, F.J. Leij, and M.Th. van Genuchten. 1995. Rapid method for estimating the unsaturated hydraulic conductivity from infiltration measurements. Soil Sci. 155:237–244.

Brooks, R.H., and A.J. Corey. 1964. Hydraulic properties of porous media. Hydrol. Paper 3, Colo. State Univ. Fort Collins, Colo.

Bruce, R.R., and A. Klute. 1956. The measurement of soil moisture diffusivity. Soil Sci. Soc. Am. Proc. 20:458–462.

Cassel, D.K., A.W. Warrick, D.R. Nielsen, and J.W. Bigger. 1968. Soil-water diffusivity values based upon time dependent soil-water content distributions. Soil Sci. Soc. Am. Proc. 32:774–777.

Clothier, B.E., D.R. Scotter, and A.E. Green. 1983. Diffusivity and one-dimensional absorption experiments. Soil Sci. Soc. Am. J. 47: 641–644.

Kirkham, D., and W.L. Powers. 1972. Advanced soil physics. Wiley Interscience, New York.

McBride, J. and R. Horton. 1985. An empirical function to describe measured water distributions from horizontal infiltration experiments. Water Resour. Res. 21:1539–1544.

Philip, J.R. 1960. General method of exact solutions of the concentration-dependent diffusion equation. Aust. J. Phys. 13:1–12.

Parlange, J.-Y. 1971. Theory of water movement in soils: 1. One-dimensional absorption. Soil Sci. 111:134–137.

Shao, M., and R. Horton. 1996. Soil water diffusivity determination by general similarity theory. Soil Sci. 161:727–734.

Warrick, A.W. 1994. Soil water diffusivity estimates from one-dimensional absorption experiments. Soil Sci. Soc. Am. J. 58:72–77.

Observations and Modeling of Profile Soil Water Storage above a Shallow Water Table

Mahmood Nachabe,* Caroline Masek, and Jayantha Obeysekera

ABSTRACT

The storage capacity of a soil profile (soil water storage capacity [SWSC]) is the depth of water required to raise a shallow water table to the land surface. The concept of SWSC is fundamental to many hydrological processes, including surface runoff by saturation excess, expansion, and contraction of wetlands, and estimation of the length of an overland flow plane. A model is introduced and tested to estimate SWSC using simultaneous observations of shallow water table fluctuations and soil moisture in a shallow, sandy soil (hyperthermic Aeric Alaquods). The water table at the selected site fluctuated between a shallow depth and the land surface during the summer, allowing frequent observation of surface inundation and profile storage. An equation of the form SWSC = $Ad^B + Cd + D$ adequately described the variability of SWSC with d, depth to the water table. It is shown that parameters A, B, C, and D are easily derived from basic physical properties of the soil horizons, including porosity and water retention. The SWSC can be significantly limited by the capillary fringe above the water table, encapsulated air (the volume of air trapped under positive pressure beneath the water table), or the presence of a clay pan at shallow soil depths. The capillary fringe had some influence on SWSC in this sandy soil, but encapsulated air as high as 11.0% of the soil volume was observed at the site. Encapsulated air reduced the available soil storage and resulted in a rapid rise in water table. Ignoring encapsulated air significantly overestimated profile storage. Storage results including and excluding air encapsulation were compared as a function of water table depth.

In humid environments, like Florida and the rest of the southeastern USA, the water table fluctuates between a shallow depth and land surface, creating a cycle of ground surface saturation recognized as the hydroperiod of an ecosystem (Ewel, 1990). Identifying the saturated zones of a landscape is needed to predict saturation excess runoff (VanderKwaak and Loague, 2001), to estimate the hydroperiod of wetlands (Arnold et al., 2001), and to determine pollutant sources from an overland flow plane (Yan and Kahawita, 2000). Recent evidence indicates that zones prone to frequent inundation and surface saturation by rising water tables contribute most of the rapid water and overland pollutant transport in the watershed. Fundamental to the identification of these variable saturation zones is the concept of SWSC, defined as the depth (volume per unit area) of water needed to raise a shallow water table to land surface. The SWSC capacity is the maximum infiltration depth that can be absorbed by the soil before the shallow water table rises to land surface initiating ponding or saturation excess overland flow.

Early observations of a quick and large response of shallow water tables were made by Meyboom (1967) and Duke (1972). Later, Gillham (1984) and Abdul and Gillham (1989) attributed this phenomenon to the high degree of saturation in the capillary fringe above the water table, resulting in a large water table rise for a small volume of water added. The ratio of added water depth to water table fluctuation is known as the specific yield of the water table aquifer (e.g., Duke, 1972). Duke (1972) introduced an equation to account for the capillary fringe influence on specific yield in a shallow water table environment. Recently, Nachabe (2002) modified the early work of Duke to account for the influence of large water table fluctuations on specific yield.

While the capillary fringe limits profile soil water storage above a shallow water table, Fayer and Hillel (1986) demonstrated that encapsulated air below the rising water table reduces further storage in the pore space. In a field study, Fayer and Hillel sprinkled water at a rate of 12.6 mm h^{-1} to bring the water table to land surface. For a fine sandy loam, they found that air encapsulation caused water table rises to be significantly higher than a soil without air encapsulation. The mechanism of air encapsulation is of significant importance to soil water storage, and was recognized in the early work of Peck (1969). Basically, when a shallow water table rises, some pores fill up before others, due to differences in velocities at the pore scale. This leads to air bubbles trapped below the water table, which are unable to escape to the atmosphere. Once encapsulated, air bubbles persist for days, even weeks, since the bubbles will dissipate from the matrix through the slow processes of dissolution or diffusion (Peck, 1969; Fayer and Hillel, 1986). Seymour (2000) surmised that large pores, particularly in sandy soils, increase the likelihood of discontinuous air bubbles being trapped in the soil matrix. This reduction in the available pore space led to the concept of water content at natural saturation because under natural recharge conditions, the soil is considered saturated although encapsulated air continues to fill a fraction of the pore space. The water content at natural saturation is the soil porosity minus encapsulated air. Wilson et al. (1982) approximated the volume of encapsulated air for one type of loamy sand as 15% of the porosity. Constantz et al. (1988) used CO_2 injection during ponded infiltration tests to measure encapsulated air. They found that encapsulated air volumes account for 19% of the porosity in medium Olympic sand (fine, mixed, active, mesic Xeric Palehumults).

In this study, we monitor the water table and the soil moisture at eight depths in a shallow Floridian sand profile. The relatively high resolution of soil moisture with depth allowed simultaneous observations of encapsulated air and SWSC above a shallow water table. The objectives of this study were (i) to introduce an equation for SWSC as a function of depth to water table, (ii) to

M. Nachabe and C. Masek, Dep. of Civil and Environmental Engineering, University of South Florida, 4202 East Fowler Avenue, ENB 118, Tampa, FL 33620; J. Obeysekera, South Florida Water Management District, West Palm Beach, FL 33406. Received 17 Mar. 2003. *Corresponding author (nachabe@eng.usf.edu).

Published in Soil Sci. Soc. Am. J. 68:719–724 (2004).

677 S. Segoe Rd., Madison, WI 53711 USA

Abbreviations: SWSC, soil water storage capacity.

assess the influences of the capillary fringe and encapsulated air on SWSC, and (iii) to test and validate the concept of SWSC with field data. The main finding of the article is that the profile soil water storage can be expressed as a polynomial function of the depth to water table. The parameters of this function can be derived from the soil hydraulic and physical characteristics. Ignoring encapsulated air below the water table may result in significant overestimation of profile water storage.

THEORY

The soil water storage equation was derived as a function of water table depth, and it incorporates physical soil hydraulic properties. For a shallow water table environment, it is customary to assume a hydrostatic, equilibrium, water content profile since the thin unsaturated zone is in close hydraulic connection with the shallow water table. This assumption has been adopted before for estimating the specific yield of shallow water table aquifers (e.g., Duke, 1972; Nachabe, 2002), and for determining soil water storage in calculating saturation excess runoff (Troch et al., 1993). In this case, the capillary pressure head is equal to elevation z above the water table. The water content distribution in a homogenous soil profile is:

$$\Theta = \left(\frac{\theta(z) - \theta_g}{\theta_s - \theta_g}\right) = \left(\frac{z}{h_A}\right)^{-\lambda} \qquad [1a]$$

for $z > h_A$, and

$$\theta = \theta_s \qquad [1b]$$

for $z \leq h_A$, where $\theta(z)$ is soil water content (m^3 of water m^{-3} of soil) at elevation z above water table (z in m is zero at water table and positive upward), θ_g is specific retention, θ_s is saturated water content, h_A is air entry pressure (in meters of water) and λ is the pore-size distribution index. The Brooks and Corey (Brooks and Corey, 1964) model of water retention is adopted in this study because representative values of its parameters have been documented in the literature, and can be easily estimated from soil texture data (e.g., Rawls et al., 1993). The maximum water depth that can be absorbed by the soil before the water table rises to the land surface is (see Fig. 1):

$$\mathrm{SWSC}(d) = \int_0^d (\theta_s - \theta(z))\mathrm{d}z \qquad [2]$$

where SWSC(d) is profile water storage (in meters), and d (in meters) is depth from the land surface to the water table. Replacing [1] in [2] and integrating yields

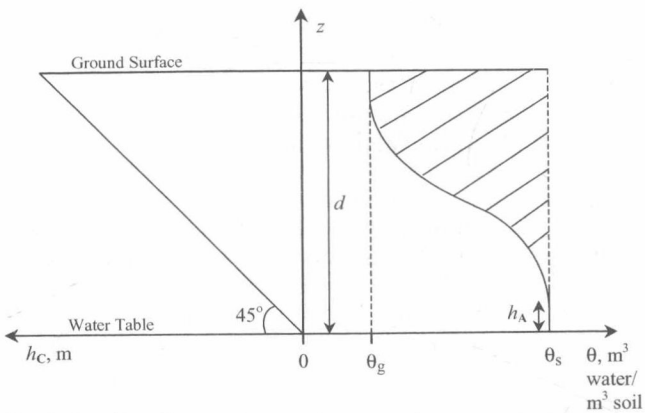

Fig. 1. Profile soil water storage above a shallow water table at depth d is represented by the hatched area.

$$\mathrm{SWSC}(d) = (\theta_s - \theta_g)\left\{(d - h_A) - \frac{h_A}{1 - \lambda}\left[\left(\frac{d}{h_A}\right)^{1-\lambda} - 1\right]\right\} \qquad [3]$$

for $d > h_A$, and SWSC(d) = 0 for $d < h_A$. The equation can be rearranged into a more convenient form such as

$$\mathrm{SWSC}(d) = \left\{-(\theta_s - \theta_g)\left(\frac{h_A}{(1 - \lambda)h_A^{1-\lambda}}\right)\right\}d^{1-\lambda} + (\theta_s - \theta_g)d + \left\{-(\theta_s - \theta_g)h_A + (\theta_s - \theta_g)\frac{h_A}{1 - \lambda}\right\} \qquad [4]$$

which is expressed as a polynomial equation:

$$\mathrm{SWSC}(d) = Ad^B + Cd + D \qquad [5]$$

where A, B, C, and D are sole functions of soil physical properties. The entire term in the left-most set of brackets in Eq. [4] is A, B is $1 - \lambda$, C is the drainable porosity ($\theta_s - \theta_g$), and D is the term in the rightmost set of brackets. This equation accommodates the influence of the capillary fringe on SWSC. For a deep water table (large d), Eq. [5] approaches a straight line with slope equal to drainable porosity. To isolate the influence of the pore-size distribution on SWSC, it is convenient to write Eq. [4] in the dimensionless form

$$I_*(d_*) = -\frac{1}{1 - \lambda}d_*^{1-\lambda} + d_* + \frac{\lambda}{1 - \lambda} \qquad [6]$$

where I_*, a normalized storage equal to SWSC/$[(\theta_s - \theta_g)h_A]$, is expressed as a function of normalized depth, d_*, equal to (d/h_A).

Equation [5] seems to capture the influence of the capillary fringe on SWSC, but this equation has not been tested before under field conditions with actual data. Also, this equation should be modified to account for encapsulated air when the water table rises to land surface. Theoretically, if encapsulated air is ignored, θ_s should be equal to the total soil porosity. The role of encapsulated air in reducing SWSC can be accommodated by treating θ_s in Eq. [2] as the water content at natural saturation, equal to porosity minus the encapsulated air volume. Currently, however, there is no systematic theory allowing estimation of encapsulated air below the water table. In this study, a field experiment was conducted to measure encapsulated air and to test the goodness of fit of Eq. [5] for profile water storage.

MATERIALS AND METHODS

The study area is in Lithia, near the planned Tampa Bay Regional Reservoir in the southeastern portion of Hillsborough County, Florida. Sandy marine sediments are the dominant parent materials for many soils in central and south Florida. The Myakka fine sand (sandy, siliceous, hyperthermic Aeric Alaquods) at this site is typical of poorly drained soil in Florida flatwoods. Carlisle et al. (1989) characterized the physical properties of Myakka fine sand, and Table 1 shows typical texture and hydraulic conductivity distributions with depth. The soil

Table 1. Soil texture, saturated hydraulic conductivity (K_s), and bulk density (D_b) with depth for Myakka fine sand, a common Florida soil.

Depth	Sand	Silt	Clay	K_s	D_b
cm		%		cm h^{-1}	g cm^{-3}
0–18	97.5	2.2	0.3	38.8	1.44
18–64	98.2	1.2	0.6	28.0	1.53
64–76	92.9	2.7	4.4	12.8	1.38
76–91	92.9	2.5	4.6	9.0	1.52
91–150	95.3	2.3	2.4	11.2	1.58
150–203	94.0	2.9	3.1	9.5	1.60

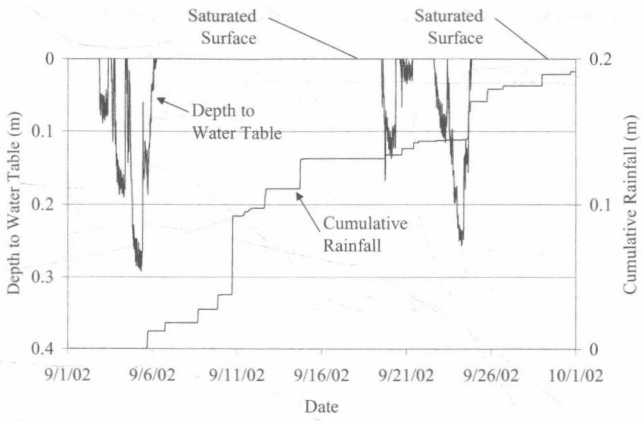

Fig. 2. Water-table depth showing periods of saturation at the land surface.

texture contains over 90% sand for all horizons, with slight variation in clay content with depth. The depth to water table at the site fluctuates between 0 and 2 m. Usually, the water table recesses to below land surface in the dry season (November through May), then gradually rises to inundate the land surface in the rainy season (June through September). Figure 2 shows the water table fluctuation at the site for a month in the wet season of 2002.

To estimate profile soil water storage and measure encapsulated air, two EnviroSCAN soil moisture probes (Sentek, Adelaide, Australia) were inserted within 30.5 m of each other. Each probe had eight soil moisture sensors placed at depths of 0.1, 0.2, 0.3, 0.4, 0.5, 0.7, 1, and 1.50 m below land surface. The sensors permitted continuous monitoring of soil moisture profiles at 5-min time intervals. The sensors use the principle of electrical capacitance (frequency-domain reflectometry) and are expected to provide volumetric water content ranging from oven dryness to saturation with a resolution of 0.1% (Buss, 1993). The default calibration equations provided by EnviroScan were used in this study. Indeed, these sensors were tested by a number of investigators in the past (e.g., Buss, 1993; Morgan et al., 1999), and more recently Fares and Alva (2000) found no significant difference in water content as measured by the probes and the gravimetric method for fine sand in central Florida. In addition to the moisture sensors, two screened water table wells recorded continuously the depth to water table every 5 min. The wells housed Instrumentation Northwest 0 to 3.45 Pa (0–5 psi) submersible pressure transducers (Instrumentation Northwest, Inc., Kirkland, WA), accurate to 34.5 Pa (0.005 psi). The wells had a total depth of 4.6 m. A typical well was made with 50.8-mm PVC pipe, with a slotted PVC screen extending below a bentonite clay seal. Silica sand was packed around the screen to allow only the passage of water.

Field Estimation of Encapsulated Air and Soil Water Storage

To illustrate how soil water storage and encapsulated air were analyzed from the data, Figure 3 shows the soil moisture profiles and the associated water table depths for a recharge (rainfall) event in which the water table raised from an initial depth of 1.37 m to a final equilibrium depth of 0.92 m below land surface. For these sandy soils, the final equilibrium water table depth is reached in about 1 d, when the water table becomes stable and ceases to exhibit any significant fluctuation with time. As expected, the soil water content is higher close to the water table (see Fig. 3) due to the capillary fringe effect, and all moisture sensors recorded an increase in water content

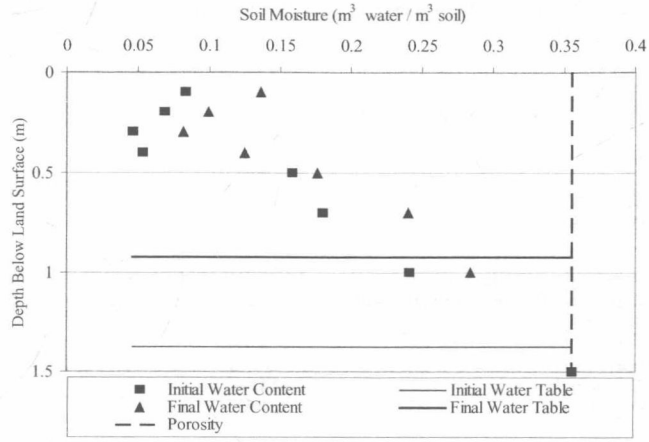

Fig. 3. Soil moisture response 2 d following a storm occurring on 22–23 Feb. 2002.

above the newly risen equilibrium water table. The submerged sensor, 1 m below the land surface, is now under the new water table but never reached full porosity (see Fig. 3). Encapsulated air volume is calculated as the porosity minus the water content measured in the submerged sensor (e.g., Fayer and Hillel, 1986).

The profile soil water storage was estimated by numerically integrating Eq. [2] with depth using the trapezoidal rule of integration. Mathematically,

$$\mathrm{SWSC}(d) = \sum_{i=1}^{n}[(\theta_{s_i} - \theta_i) + (\theta_{s_{i+1}} - \theta_{i+1})]\Delta z_i/2 \quad [7]$$

where θ_i is the recorded water content by the sensor at elevation i, θ_{si} is the saturated water content (equal to full porosity, if encapsulated air is neglected, or porosity minus encapsulated air, if encapsulated air is accounted for), and Δz_i is elevation distance between the moisture sensors i and $i + 1$. Calculations of SWSC are repeated for different values of d in Eq. [7]. Finally, Eq. [4] was fitted using regression to this SWSC(d) data to test the goodness of fit of this model to field observations.

In most practical applications, however, field observations from soil moisture probes will not be available to develop the SWSC(d) relationship. In this case, one has to use readily available soil water retention data $\theta(h_C)$ for $\theta(z)$ in Eq. [7]. To test this approach, water retention data for two Floridian soils were selected: Immokalee fine sand (siliceous, hyperthermic Arenic Alaquod) and Smyrna sand (Sandy, siliceous hyperthermic Aeric Alaquod). Water retention characteristics were obtained from duplicate undisturbed soil cores placed in Tempe pressure cells (Soil Measurement Systems, Tucson, AZ), saturated and then extracted at different capillary pressures (Carlisle et al., 1989). Table 2 summarizes the soil water retention for these two soils. Once SWSC data from Eq. [7] were calculated, we fitted Eq. [4] to this data using a least squares regression technique.

RESULTS AND DISCUSSION

Effect of the Capillary Fringe on the Soil Water Storage Capacity Equation

The capillary fringe reduces the available water storage above a shallow water table, a behavior that can be captured by Eq. [4], which relates storage to depth to water table. Figure 4 shows a plot of the normalized storage I_* versus d_* for three values of λ. Theoretically,

Table 2. Water retention data for Immokalee fine sand and Smyrna sand, and soil texture, saturated hydraulic conductivity, and bulk density.

				Immokalee fine sand				
Capillary pressure, m	0.035	0.20	0.30	0.45	0.60	0.80	1.50	2.00
Water content, m^3 water m^{-3} soil	0.378	0.353	0.352	0.242	0.156	0.086	0.051	0.049
Sand, %	98.7							
Silt, %	0.8							
Clay, %	0.5							
K_s, cm h^{-1}	20.4							
D_b, g cm^{-3}	1.44							
				Smyrna sand				
Capillary pressure, m	0.035	0.20	0.30	0.45	0.60	0.80	1.50	2.00
Water content, m^3 water m^{-3} soil	0.337	0.320	0.317	0.292	0.177	0.122	0.059	0.048
Sand, %	97.1							
Silt, %	2.3							
Clay, %	0.6							
K_s, cm h^{-1}	14.8							
D_b, g cm^{-3}	1.51							

SWSC remains zero for water table depth less than the air entry pressure, then the SWSC asymptotically approaches a straight line as the water table gets deeper. Indeed, by taking the derivative of Eq. [4], the slope of the SWSC(d) relationship approaches the drainable porosity, $(\theta_s - \theta_g)$, as d increases. For shallow water table environments, soils with a narrow pore-size distribution (large λ) have more SWSC than soils with a wide pore-size distribution (small λ). Also for all soil types, the influence of the capillary fringe seems limited to elevations of about $3h_A$ above the water table (see Fig. 4). In hydrological applications, like the estimation of water balances for wetlands, one is usually interested in shallow water table environments; therefore the capillary fringe is likely to play a significant role in reducing profile storage in these environments.

Figure 5 shows the fit of Eq. [5] to the SWSC of Immokalee and Smyrna sands calculated through water retention data. Equation [5] provided a very good fit for storage with $r^2 = 0.99$ for both soils. The regression constants for Eq. [5] for the Smyrna sand were $A = 233$, $B = -0.015$, $C = 0.41$, and $D = -229$ while the constants for the Immokalee fine sand were $A = 147$, $B = -0.024$, $C = 0.45$, and $D = -144$. The two soils had a pore-size distribution index slightly larger than one ($\lambda = 1 - B$), reflective of fine sandy soils (e.g., Brooks and Corey, 1964). The drainable porosity for Immokalee fine sand (0.45) was larger than the drainable porosity for Smyrna sand (0.41), and that resulted in a steeper slope for SWSC(d) for deep water tables (large d values). If the influence of the capillary fringe is neglected, then one might erroneously consider that the volume of water to fill the soil storage would be depth to water table multiplied by the drainable porosity. For $d = 0.50$ m, one would then predict that the SWSC for Smyrna sand is $0.50 \times 0.41 = 0.205$ m, whereas the storage, taking into account the influence of the capillary fringe, is <0.07 m at this depth. Clearly, the influence of the capillary fringe on SWSC cannot be ignored. The goodness of fit of Eq. [4] is encouraging because soil water retention characteristics are documented in numerous references and are more readily available.

Effect of Air Encapsulation on the Soil Water Storage Capacity Equation

Soil water retention data, however, are often determined in the laboratory under drainage conditions, and do not account for encapsulated air below a rising water table. Table 3 presents the average and the standard deviation of the observed air encapsulation at the eight moisture sensors on each probe. The averages were cal-

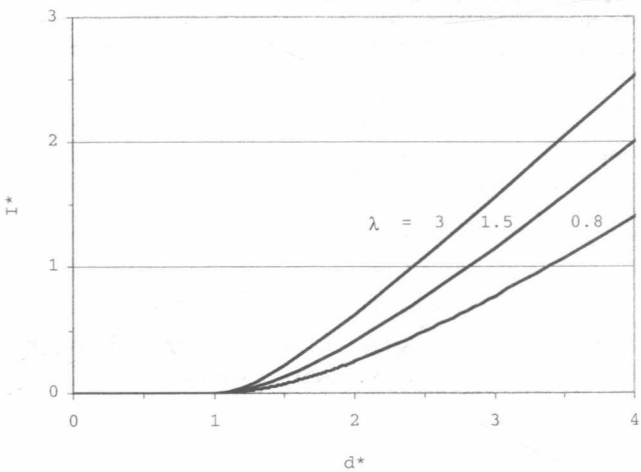

Fig. 4. Dimensionless soil water storage capacity (SWSC) equation where I_* equals the normalized soil storage and d_* equals the normalized water-table depth.

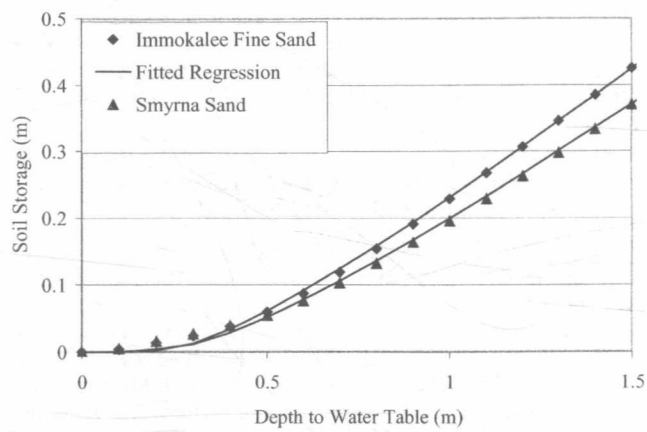

Fig. 5. The soil water storage capacity (SWSC) equation applied to two Floridian soils. The SWSC was estimated through the numerical integration of Eq. [2] using water retention data. The solid lines show the fit of Eq. [5] to these data.

Table 3. Air encapsulation volume as a function of depth below land surface.

Depth below land surface, m	.20	.30	.40	.50	.60	.70	.90	1.0	1.10	1.20
Volumetric encapsulated air, %	2.6	6.5	11.0	9.2	–	9.6	9.8	8.7	3.4	–
Fayer and Hillel (1986) volumetric encapsulated air, %	–	4.8	–	–	6.3	–	4.7	–	–	1.7

culated from 1 to 4 measurements during different recharge events for each sensor depth. For the sake of comparison, the volumetric encapsulated air determined by Fayer and Hillel (1986) for a sandy loam soil was also included in this table. These latter values are somewhat smaller than those measured during our experiment, which might be attributed to soil texture differences and the high fraction of sand in Florida. Encapsulated air volumes at the site increased with depth up to a maximum of 11% at 0.40 m below the land surface, then decreased for greater depths. Similar behavior was observed for the data provided by Fayer and Hillel (1986). The relatively small value of encapsulated air at 0.20 m below land surface could be attributed to proximity from land surface, which facilitates the escape of air.

To assess the influence of encapsulated air on SWSC, porosity was adjusted using the encapsulated air volumes in Table 3. Figure 6 compares the SWSC(d) optimized fit using Eq. [5], with and without correction for encapsulated air. Encapsulated air reduced significantly the profile water storage capacity. For example, with the encapsulated air effect included, it takes only 0.07 m of water to raise the water table from a depth of 0.75 m to land surface (see Fig. 6). A SWSC equation that ignores encapsulated air would predict that 0.12 m of water would be needed to bring the water table to land surface, an over prediction of over 70%. These differences are large considering a water budget for a wetland or for estimating variable saturation areas.

Field Estimated Soil Water Storage

In this section, we compare profile storage calculated from the sensors on the moisture probes with the storage calculated from retention data. Figure 7 shows the fit with Eq. [5], while neglecting encapsulated air (full porosity is used in Eq. [7]). Although the fit is reasonable with an r^2 of 0.88, the scatter around the curve can be attributed to at least two reasons. Equation [5] was developed assuming a homogenous soil profile and an equilibrium water content distribution. Both assumptions are not completely realistic in field conditions. The Myakka fine sand at this site had a fairly uniform soil texture profile with depth, which is typical of Florida's undeveloped soils. In well-developed soils, leaching of clay minerals over time may result in clear textural differences or clay pans at shallow depth, which may limit further the applicability of Eq. [5].

Figure 8 shows the fit of the model to profile storage calculated from retention data after correcting for encapsulated air. Profile storage calculated from moisture sensors and corrected for air encapsulation is superimposed. The fit of Eq. [5] dropped to 0.75 when encapsulated air is considered. The increase in scatter around the fit can be attributed to the nonuniformity of encapsulated air with depth, which increases the variability of the water content at natural saturation (porosity minus encapsulated air). It is difficult to speculate on the physical mechanisms responsible for the large variability of encapsulated air with depth. During water table rise, microscopic variability in water velocity causes pores to fill before others, a phenomenon that isolates and traps air bubbles (e.g., Peck, 1969). Thus depending on the rate of recharge and water table rise, different volumes of air bubbles can be encapsulated. Other reasons that may influence variability with depth are soil textural differences in the profile, and proximity from land surface.

The regression parameters for Eq. [5] including and excluding the effects of encapsulated air, are presented in Table 4. The values of the Brooks–Corey parameters are obtained from the knowledge of their relationships to these regression parameters (see Eq. [4] and [5]), and are thus considered effective parameters for the profile. The pore-size distribution remained essentially the same whether encapsulated air was included or excluded from the regression fit. Inclusion of encapsulated air, however, increased the effective air entry pressure and reduced the effective drainable porosity. As expected, a

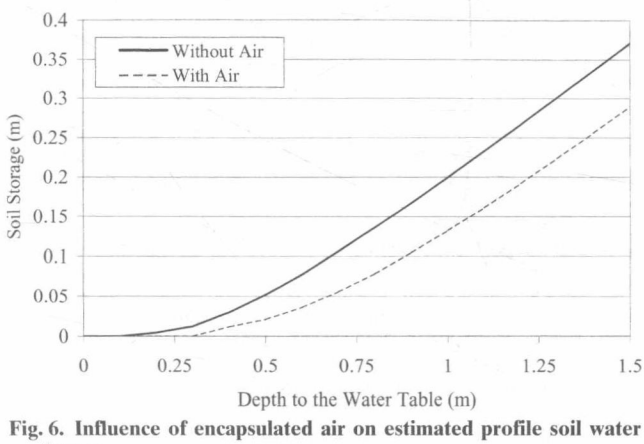

Fig. 6. Influence of encapsulated air on estimated profile soil water storage.

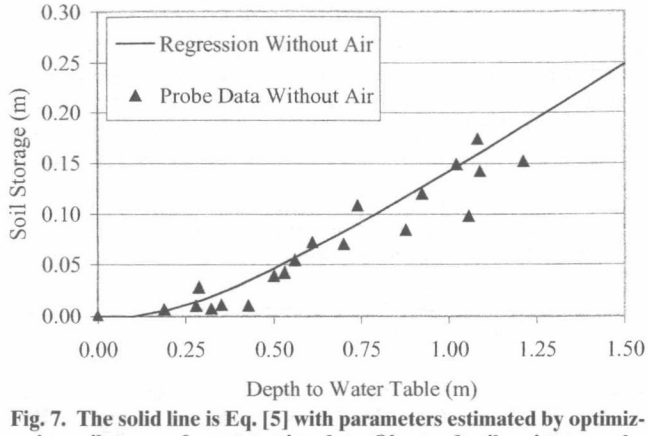

Fig. 7. The solid line is Eq. [5] with parameters estimated by optimizing soil storage from retention data. Observed soil moisture probe storages (triangles) without correction for air are superimposed.

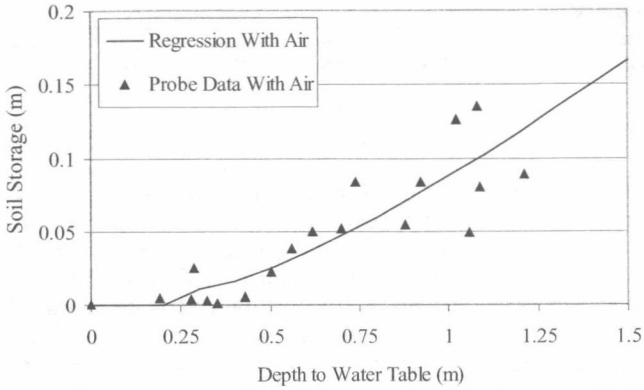

Fig. 8. Equation [5] is optimized fit after correcting for air encapsulation. Observed soil moisture probe storages with correction for air are superimposed.

higher air-entry pressure and a lower drainable porosity tend to reduce the profile soil water storage.

CONCLUSIONS

The objective of this study was to introduce and test an equation to estimate the profile soil water storage above a shallow water table. Estimation of this storage is needed for prediction of variable saturation areas, which are prone to seasonal flooding by rising water tables. There is a growing awareness of the need to identify these critical areas to control pollutant transport by saturation excess overland flow.

Estimation of profile soil water storage is complicated by encapsulated air, the capillary fringe, and soil texture heterogeneity. Both the capillary fringe and encapsulated air act to reduce the profile soil water storage. Use of drainable porosity may substantially overestimate profile storage. While we have reproduced some representative values for encapsulated air in a sandy profile, encapsulated air varied substantially with depth. Future research should work on developing a coherent theory that allows better quantification of the physical mechanisms responsible for encapsulated air below rising water tables.

A simple equation was introduced to simulate profile water storage above the water table in a sandy profile. This equation assumes that (i) the soil profile is homogenous, and (ii) the water content distribution is at equilibrium. Although this equation seemed to fit reasonably well profile storage in this homogenous sand profile, it is unlikely that it remains valid in profiles where soil horizons exhibit sharp contrast in their texture (e.g., a clay pan at shallow depth). The profile storage equation is physically based, and the regression constants could be derived for a number of common soils using retention data. This should facilitate its use by practitioners. The equation was tested with field data and seemed to capture reasonably well the influence of capillary fringe on profile water storage. Correcting for encapsulated air, however, was necessary to simulate profile storage under natural recharge conditions.

Table 4. Brooks and Corey parameters derived from regression constants using Eq. [5] after optimization both without and with inclusion of air encapsulation.

Without air encapsulation					With air encapsulation				
λ		h_A		$\theta_s - \theta_g$	λ		h_A		$\theta_s - \theta_g$
		cm					cm		
0.959		14.5		0.243	0.955		25.4		0.199
A	B		C	D	A	B		C	D
−31.6	0.041		0.24	32.7	−39.5	0.045		0.20	42.2

ACKNOWLEDGMENTS

Funding for this work was provided by South Florida Water Management District (contract #C-13382) and the National Research Initiative Competitive Grant Program/USDA (CSREES award #2001-35102-10829). M. Nachabe is the PI on both awards.

REFERENCES

Abdul, A.S., and R.W. Gillham. 1989. Field studies of the effects of the capillary fringe on streamflow generation. J. Hydrology (Amsterdam) 112:1–18.

Arnold, J.G., P.M. Allen, and D.S. Morgan. 2001. Hydrologic model for design and constructed wetlands. Wetlands 21:167–178.

Brooks, R.H., and A.T. Corey. 1964. Hydraulic properties of porous media. Hydrology Paper 3. Colorado State University, Fort Collins.

Buss, P. 1993. The Use of capacitance based measurements of real time soil water profile dynamics for irrigation scheduling. Proc. Natl. Conf. Irrig. Assoc., Australia and Natl. Comm. Irrig. Drain., Launceston, Tasmania, 17–19 May 1993. Irrig. Assoc. Austr., Homebush, NSW.

Carlisle, V.W., F. Sodek, M. Collin, L.C. Hammond, and W.G. Harris. 1989. Characterization data for selected Florida soils. Institute of Food and Agricultural Sciences, University of Florida, Gainesville.

Constantz, J., W.N. Herkelrath, and F. Murphy. 1988. Air encapsulation during infiltration. Soil Sci. Soc. Am. J. 52:10–16.

Duke, H.R. 1972. Capillary properties of soils-influence upon specific yield. Trans. ASAE 688–699.

Ewel, K. 1990. Swamps. p. 281–323. *In* R.L. Myers and J.E. Ewel (ed.) Ecosystems of Florida, University of Central Florida Press, Orlando.

Fares, A., and A.K. Alva. 2000. Evaluation of capacitance probes for optimal irrigation of citrus through soil moisture monitoring in an Entisol Profile. Irrig. Sci. 19:57–64.

Fayer, M.J., and D. Hillel. 1986. Air encapsulation: I. Measurement in a field soil. Soil Sci. Soc. Am. J. 50:568–572.

Gillham, R.W. 1984. The Capillary fringe and its effect on water-table response. J. Hydrology (Amsterdam) 67:307–324.

Meyboom, P. 1967. Ground water studies in the Assiniboine river drainage basin, II, Hydrologic characteristics of phreatophytic vegetation in south-central Saskatchewan. Geol. Surv. Can. Bull. 139:64.

Morgan, K.T., L.R. Parsons, T.A. Wheaton, D.J. Pitts, and T.A. Obreza. 1999. Field calibration of a capacitance water content probe in fine sand soils. Soil Sci. Soc. Am. J. 63:987–989.

Nachabe, M.H. 2002. Analytical expressions for transient specific yield and shallow water table drainage. Water Resour. Res. 38:1193 10.1029/2001WR001071.

Peck, A.J. 1969. Entrapment, stability, and persistence of sir bubbles in soil water. Aust. J. Soil Res. 7:79–90.

Rawls, W. J., L.R. Ahuja, D. Brakensiek, and A. Shirmohammadi. 1993. Infiltration and soil water movement. p. 5.1–5.51. *In* D. Maidment (ed.) Handbook of hydrology. McGraw-Hill, New York.

Seymour, R.M. 2000. Air entrapment and consolidation occurring with saturated hydraulic conductivity changes with intermittent wetting. Irrig. Sci. 20:9–14.

Troch, P.A., M. Mancini, C. Paniconi, and E.F. Wood. 1993. Evaluation of a distributed catchment scale water balance model. Water Resour. Res. 29:1805–1818.

VanderKwaak, J.E., and K. Loague. 2001. Hydrologic-Response simulations for the R-5 catchment with a comprehensive physics-based model. Water Resour. Res. 37:999–1013.

Wilson, B.N. D.C. Clack, and R.A. Young. 1982. A comparison of three infiltration models. Trans. ASAE 25:349–356.

Yan, M., and R. Kahawita. 2000. Modeling the fate of pollutant in overland flow. Water Res. 34:3335–3344.

Aggregate-Size Stability Distribution and Soil Stability

C. O. Márquez,* V. J. Garcia, C. A. Cambardella, R. C. Schultz, and T. M. Isenhart

ABSTRACT

A new theoretical and experimental framework that permits an accurate determination of aggregate-size stability distribution is presented. The size-stability distribution in addition to estimating aggregate-size distribution distinguishes between amounts of stable and unstable macroaggregates (>250 μm). The determination of aggregate-size stability distribution involves the assumptions that soil aggregates can be categorized in terms of their size and water stability (slaking resistance). Experimentally this procedure involves the slaked and capillary-wetted pretreatments; and a subsequent slaking treatment of aggregates >250 μm in size. We also propose the stable aggregates index (SAI) and the stable macroaggregates index (SMaI) for studying soil stability based on aggregate resistance to slaking. These indices account for the total weighted average of stable aggregates and the total weighted average of stable macroaggregates, respectively. Both the SAI and the SMaI indices were shown to be sensitive to the effects of vegetation on soil stability under different riparian buffer communities. The SAI and the SMaI indices were higher in surface soils under cool-season grass than any of the other treatments. These soils samples are well aggregated with SAI = 74% and SMaI = 56% followed by SAI = 55% and SMaI = 37% under existing riparian forest, SAI = 40% and SMaI = 21% under 7-yr switchgrass and SAI = 36% and SMaI = 18% under cropped system.

Soil aggregate stability is the result of complex interactions among biological, chemical, and physical processes in the soil (Tisdall and Oades, 1982). Factors affecting aggregate stability can be grouped as abiotic (clay minerals, sesquioxides, exchangeable cations), biotic (soil organic matter, activities of plant roots, soil fauna, and microorganisms), and environmental (soil temperature and moisture) (Chen et al., 1998). The concept of aggregate stability depends on both the forces that bind particles together and the nature and magnitude of the disruptive stress (Beare and Bruce, 1993).

Several methods have been proposed to determine soil aggregate-size distribution and stability (Kemper and Rosenau, 1986). The suitability of these methods depends on the purpose of the study. The most widely used approaches are based on the wet-sieving method (Kemper, 1966; Kemper and Rosenau, 1986). In this method, cyclically submerging and sieving soil in water emulates the natural stresses involved in the entry of water into soil aggregates. The moisture content of the soil aggregates before wet sieving controls the severity of the disruption (Kemper and Rosenau, 1986). Several studies have used capillary-wetted and slaked pretreatments (Elliott, 1986; Cambardella and Elliott, 1993a; Six et al., 1998) as a means to study soil aggregates. The capillary-wetted pretreatment involves slowly wetting the soil aggregates before wet sieving. This pretreatment produces minimal disruption, because misted aggregates do not buildup air pressure in the pores and the air escapes with minimal aggregate disruption. In contrast, the slaked pretreatment causes considerable disruption. When air-dry soil is submerged in water; the air that is trapped inside the soil pores is rapidly displaced with water. Weak aggregates are disrupted as a consequence of the sudden release of this large buildup of internal air pressure (Cambardella and Elliott, 1993a; Gale et al., 2000).

The combined use of the capillary-wetted and the slaked pretreatments has been used for contrasting differences in aggregate-size distributions for soils with different management histories and also for understanding the factors that influence aggregate stability (Elliott, 1986; Cambardella and Elliott, 1993a; Six et al., 1998). More recently, Gale et al. (2000) used the comparison of slaked versus capillary-wetted pretreatments as a means to differentiate stable macroaggregates from unstable macroaggregates based on their resistance to slaking. Although the conceptualization of Gale's idea represents an important contribution, more work is needed to clearly separate the stable macroaggregates from the unstable macroaggregates and accurately specify aggregate-size stability distributions. The aggregate-size stability distribution is the quantity of stable and unstable soil aggregates categorized by their size and stability to disruption.

Existing approaches for studying soil aggregates do not fully distinguish between stable and unstable aggregates based on their resistance to slaking. In turn, this causes significant errors in assessing soil stability by the wet-sieve method and the dynamics of soil aggregates and the C associated with aggregates. The disruption of unstable macroaggregates during the slaking treatment produces smaller constituent aggregates that are accounted for in smaller aggregate-size fractions biasing the aggregate-size distribution. In contrast, the capillary-wetted pretreatment does not account for differences in stable and unstable macroaggregates because of the lack of violent disruption.

We hypothesize that using a subsequent slaking of the capillary-wetted soil in addition to the slaking and capillary-wetted pretreatments should yield a more accurate determination of the amount of stable and unstable macroaggregates. This in turn can be used to determine the aggregate-size stability distribution. This

C.O. Márquez, Facultad de Ciencias Forestales y Ambientales, Universidad de los Andes, Mérida, Venezuela; V.J. García, Dep. de Física, Facultad de Ciencias, Universidad de los Andes, Mérida, Venezuela; C.A. Cambardella, USDA-ARS, National Soil Tilth Lab., 2150 Pammel Dr., Ames, IA 50011; R.C. Schultz and T.M. Isenhart, Dep. of Natural Resource Ecology and Management, Iowa State University, Ames, IA 50011. Received 27 Mar. 2003. *Corresponding author (omarquez@ula.ve).

Published in Soil Sci. Soc. Am. J. 68:725–735 (2004).

677 S. Segoe Rd., Madison, WI 53711 USA

Abbreviations: SAI, stable aggregates index; SMaI, stable macroaggregates index.